Optical Heterodyne Detected Accumulated Acoustic Grating Responses in Near Supercritical Fluids

Jian Peng and Lawrence D. Ziegler*

Department of Chemistry and The Photonics Center, Boston University, Boston, Massachusetts 02215

Received: September 6, 2007; In Final Form: October 11, 2007

A novel third-order polarization effect due to an accumulated optical heterodyne detected (OHD) transient acoustic grating response in near critical fluids was observed and experimentally characterized. Femtosecond pump−probe responses in near critical CO_2 and CHF_3 illustrate this phenomenon. This large optically generated acoustic response due to electrostrictive coupling appears only when pump and probe pulses are temporally overlapped and is π out-of-phase with the normal optical Kerr effect (OKE) birefringent signal. The local oscillator, the laser intensity, and the modeled experimental repetition rate dependence identify the accumulated heterodyne origin of these responses. The observed OHD accumulated acoustic birefringent signal is inversely dependent on sound velocity to the fifth power. A corresponding sound velocity dependent dichroic (in-phase) response was also observed for these electronically nonresonant samples. The accumulated effect described here may have applications for the design of efficient modulators and as a simple and sensitive experimental technique for the measurement of near critical fluid thermodynamic and acoustic parameters.

Introduction

The ability of optical pulses to write and read transient acoustic gratings has been exploited over the past 30 years to learn about sound propagation and attenuation, material structural characterization, weak absorptions, and thermal diffusion in solids, liquids, and gases.[1−7] In one well-studied experimental arrangement for the observation of optically excited acoustic responses, two optical pulses from the same laser source at a carrier wavelength λ_{exc} intersect at an angle θ with respect to each other and temporally and spatially overlap in a sample. The simultaneous spatial overlap of the electric fields of the two laser beams creates an intensity interference pattern in the material, producing a fringe spacing, Λ, given by

$$\Lambda = \frac{\lambda_{exc}}{2\sin(\theta/2)} \quad (1)$$

This periodic spatial intensity pattern results in counter propagating acoustic standing waves due to density changes arising from rapid thermal expansion or electrostriction forces depending on whether the sample is absorbing or transparent at λ_{exc}, respectively. For the typical experimental parameters employed in this study ($\lambda_{exc} = \sim$800 nm and $\theta = 8°$), Λ corresponds to an angular acoustic frequency (ω) of ∼200 MHz. A time delayed probe pulse incident on the grating, at some different angle and often at some new color, is reflected into a detector at an angle that satisfies the Bragg reflection condition. When the delay between the probe and the pair of excitation or pump pulses is scanned, the time dependence of the generally underdamped acoustic response, or more properly the square of this quantity, is observed.[2−4] This transient grating interaction can be described in a third-order nonlinear polarization, $P^{(3)}(t)$, framework, and the resulting signal in this typical experimental configuration is thus a homodyne response, $|P^{(3)}(t)|$.[2] When a sufficiently intense additional local oscillator field ($|E_{LO}| \gg |P^{(3)}|$) is temporally and spatially overlapped with the $P^{(3)}(t)$ derived signal field, the optically excited acoustic response can also be heterodyne detected.[8] Longitudinal acoustic waves can also be optically generated by strain waves resulting from rapid heating in thin films.[9] Here, we report a new manifestation of optically generated acoustic responses that are only clearly evident in a special class of fluids: near supercritical fluids (SCFs). The purpose of this paper is to provide a detailed experimental characterization of this novel nonlinear effect in near SCFs that identifies the origin of these signals, contrasts their observation in normal liquids, and indicates potential applications for this phenomenon. The samples of study here are near critical CO_2 and CHF_3 fluids. Both CO_2 and CHF_3 have experimentally convenient critical state points (see Table 1): $P_C = 72.8$ atm and $T_C = 31.1$ °C for CO_2 and $P_C = 47.7$ atm and $T_C = 25.6$ °C for CHF_3.

During recent studies of the decays of the H_2 rotational Raman resonances in near supercritical (SC) CO_2, which act as a probe of the anisotropic fluctuation dynamics in this solvent,[10] we observed an anomalous feature in the ultrafast optical heterodyne detected (OHD) optical Kerr effect (OKE) responses of H_2/CO_2 near critical solutions. In this standard OHD−OKE two-beam experimental configuration,[11] a large autocorrelation-shaped feature centered at the $t = 0$ pump−probe temporal overlap region appeared in these OHD−OKE responses of SC H_2/CO_2 mixture fluids. This feature was strongly density dependent, increasing in strength as the critical point was approached and was π out-of-phase with the normal nonresonant electronic and Raman nuclear responses of the H_2/CO_2 mixture, which remained virtually unchanged over the same temperature region. This effect is illustrated in Figure 1 for a 25% (mol fraction) mixture of H_2 in SC CO_2 obtained with the 76 MHz 22 fs output of a Ti:sapphire oscillator in the standard two-beam OHD configuration.[11] The critical temperature for this H_2 solution (CO_2 density = 0.8 ρ_C) is reduced by ∼10 to ∼21 °C from the neat CO_2 T_C. Such density dependent features in the region of the nonresonant electronic response were not

* Corresponding author. E-mail: lziegler@bu.edu.

10.1021/jp0771771 CCC: $37.00
Published on Web 12/01/2007

TABLE 1: Sound Velocity and Attenuation for CO_2, CHF_3, and $CHCl_3$ at Various State Points

substance	phase	density (ρ/ρ_C)	temp (K)	sound velocity (m/s)[a]	sound attenuation α/ν^2 (s^2 m^{-1})
CHF_3	SC	1.2	306	146	$\sim 4 \times 10^{-11}$ (ref 5)
$T_C = 299.3$ K and $P_C = 47.7$ atm	liquid	1.5	294	183	
$\rho_C = 7.52$ M					
CO_2	SC	0.8	308	185	$\sim 10^{-10}$ (ref 17)
$T_C = 304.1$ K and $P_C = 72.8$ atm	liquid	1.7	293	350	
$\rho_C = 10.6$ M					
$CHCl_3$	liquid	2.99	295	995	8.8×10^{-13} (ref 4)
$T_C = 537$ K and $P_C = 52.6$ atm					

[a] CHF_3 and CO_2 sound velocities from ref 14, and $CHCl_3$ sound velocity from ref 33.

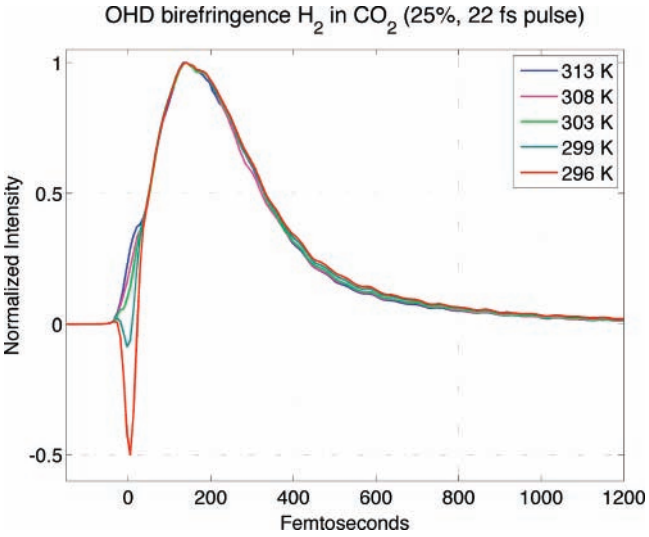

Figure 1. Birefringent responses of a mixture of 25% H_2 in CO_2, $\rho^* = 0.8$ as a function of temperature in the vicinity of the critical point. $T_C \cong 293$ K for this mixture.

observed in a previous OHD ultrafast study of the birefringent responses of CO_2 at virtually identical near critical state points using 50 fs pulses at ~600 nm from an regeneratively amplified Ti:sapphire laser system operating at 100 kHz.[12] As will be shown below the novel time dependent feature observed in the ultrafast OHD responses of the near SCFs studied is due to accumulated, optical heterodyne detected acoustic transient gratings and its prominent appearance in the samples of interest here is attributable to the unique properties of fluids near the SC region as compared to normal liquids.

Probably the key material property responsible for the appearance of the acoustic responses reported here is the isothermal compressibility as it relates to the speed of sound, υ_S, in these fluids. The thermodynamics based expression for the sound velocity in a fluid at temperature T, υ_S (low-frequency limit) is[13]

$$\upsilon_S = V\left(\frac{T}{MC_V}\right)^{1/2}\left(\frac{\partial P}{\partial T}\right)_V\left[1 - \frac{C_V}{T}\frac{(\partial P/\partial V)_T}{(\partial P/\partial T)_V{}^2}\right]^{1/2} \qquad (2)$$

where V is the molar volume, M the molar mass, and C_V the constant volume molar heat capacity. At the critical point, $C_P \rightarrow \infty$ ($\gamma \equiv C_P/C_V \rightarrow \infty$), and the inverse compressibility, $V(\partial P/\partial V)_T$, vanishes. Thus, the sound velocity is a minimum at the critical point. The temperature dependent υ_S values for CO_2 and CHF_3 in the critical point region given by equations of state are plotted in Figure 2[14] and illustrate the effects of this singularity. Corresponding experimental sound velocities for the normal liquids $CHCl_3$ and CH_3CH_2OH,[15] also shown in Figure 2, are about an order of magnitude faster than that of the critical fluids. This υ_S minimum at the critical point is well-known experimentally and has been observed in SC CO_2 and CHF_3 acoustic studies.[5,16−18]

In addition to υ_S, another important parameter affecting acoustic grating based optical responses is the acoustic attenuation rate in a given material. Sound attenuation (acoustic energy loss) in molecular fluids can be attributed to the effects of shear viscosity, thermal conductivity, and translation to rotation and vibration energy transfer.[19] The sound absorption coefficient, α (Np m^{-1}), can be defined in terms of the sound velocity by

$$\alpha = 1/\tau_a\upsilon_S \qquad (3)$$

where τ_a^{-1} is the damping rate constant for the acoustic wave (i.e., the acoustic amplitude is proportional to $\exp(-t/\tau_a)$). The sound absorption coefficient normalized by the square of the acoustic frequency, α/ν^2, is a constant for many fluids and generally is the experimentally reported quantity in sound absorption measurements.[18,20] In particular, this quantity has been shown to be a constant for SC CHF_3 in the frequency range of interest here ($\omega = 2\pi\nu = \sim 200$ MHz).[5] Very near the critical point ($T_C \pm 0.5$ K), α/ν^2 dramatically increases[16,18] due to the γ (C_P/C_V) weighted thermal conductivity contribution to the acoustic absorption as found in the classical Stokes−Kirchhoff attenuation expression.[18]

Finally, in anticipation of the phenomenon reported here, we note that accumulated nonlinear responses, due to the buildup of optically pumped steady state transient populations, have been observed in a number of experimental studies employing high repetition rate laser excitation.[21−25] Accumulated $P^{(3)}$ based responses have been reported in the observation of photon echo signals generated in solid state materials where the buildup of accumulated population gratings occurs due to a bottleneck state whose lifetime is greater than the time between successive excitation pulses. The resulting accumulated photon echo signal is necessarily an optical heterodyne detected response. Of greater relevance to the signals reported here, a thermally generated accumulated phase grating generated a symmetric autocorrelation-shaped response in the pump−probe response of a rapidly flowing resonant dye solution. The phase shift allowing this optical response to be observed in the inherently dichroic heterodyne experimental configuration employing a high repletion rate (83 MHz) laser system was attributed to the sample motion during the slow thermal relaxation time.[25] The magnitude and sign of those dichroic signals based on the real part of the sample's $P^{(3)}$ response could be controlled by adjusting the flow direction of the sample jet relative to the grating **q** vector. The SCF signals described here exhibit features that are analogous to these thermally generated phase grating responses.

Experimental Procedures

Sample Preparation. OHD−OKE/pump−probe measurements were performed on fluid samples contained in a stainless steel optical cell, between a pair of 6.3 mm thick fused silica

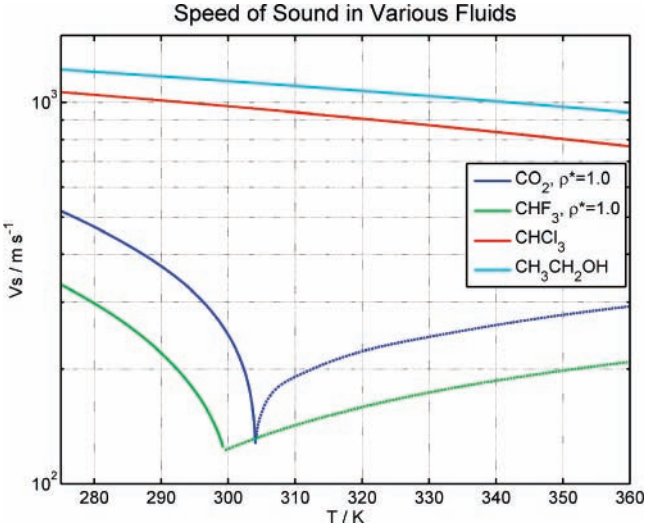

Figure 2. Semilog plot of the temperature dependence of the speed of sound[14] in the vicinity of the critical points of CO_2 and CHF_3 (at the critical density, $\rho^* = 1$). The speed of sound in normal liquids $CHCl_3$ and CH_3CH_2OH in this temperature range[15] is shown for comparison as well. The dashed lines correspond to the SC fluid phase.

windows spaced 5.5 mm apart. High-pressure seals were provided by PTFE O-rings to reduce potential contamination associated with SC extraction. An electrical rope heater (FGR, Omega Engineering, Inc.) was judiciously wrapped around the optical cell to minimize temperature gradients. The cell temperature was monitored with surface-mounted thermocouples and regulated with a PID controller (CN77323, Omega Engineering, Inc.) to within ±0.1 K. High-pressure fluids (CHF_3 99.95%, CO_2 99.996%, Linde Gas U.S.A. LLC) were compressed into the optical cell with a pressure generator (HiP 87-6-5). The cell pressure was measured with a thin-film transducer (PX 602, Omega Engineering, Inc.) with a precision of ±1 psi.

To prepare the SC samples, both the optical cell and the high-pressure generator were heated to 15 K above the critical temperature, so that no phase separation occurred during the isothermal compression. After the desired amount of fluid was delivered into the optical cell, it was disconnected from the pressure generator and gradually cooled down to the desired temperature. The fluid samples were then allowed to equilibrate before any spectroscopic measurements were taken.

Laser Configuration. Ultrafast responses were obtained in a two-beam pump−probe setup or a standard two-beam optical heterodyne detected OKE configuration.[11,12] As is usual in this OKE configuration, anisotropic dichroic signals (in-phase, $\phi_{LO} = 0$) were obtained by rotating an analyzing polarizer between the sample and the detector, and birefringent ($\pi/2$ out-of-phase, $\phi_{LO} = \pi/2$) signals resulted when the polarizer in front of a quarter wave plate in the probe arm was rotated. Ti:sapphire oscillator pulses at 76 MHz and a variety of pulse widths in the range of 20−45 fs were used to observe the accumulated signals reported here. Typically, 1.5 nj pulses at ∼800 nm were focused to a ∼50 μm spot by a 15 cm lens. Pump and probe beam intensities were nearly equal and crossed at angles in the range of 4 to 8° in the sample. The pump was chopped at 1.4 kHz. For double chopping experiments, the pump and probe beams were modulated at 1.4 and 1.0 kHz, respectively. A Conoptics (model 25D) pulse picker was used to make OHD and pump−probe measurements at pulse repletion rates below 76 MHz from our Ti:sapphire oscillator. At the near critical state points examined here, spurious scattered incident pump light from the SCF did not interfere with the observation of these OHD signals.

Results and Discussion

Phenomenological Overview. As discussed previously, a prominent feature was observed in the two-beam, one-color OHD pump−probe birefringent responses of CO_2 and CHF_3 near the critical point excited and probed by the ∼25 fs pulse output of a Ti:sapphire oscillator (∼795 nm) operating at 76 MHz only when the two pulses were temporally overlapped. As seen in Figure 1, this density dependent contribution had the time dependence of the intensity autocorrelation function and was π out-of-phase with the standard nonresonant electronic and Raman coupled nuclear responses. The phase (sign) of this feature was controlled by the relative phase (sign) of the local oscillator (LO) field in this birefringent OHD−OKE configuration.[11] No other significant changes were observed outside of the region where the pump and probe pulse temporally overlapped (see Figure 1) as the SC CO_2/H_2 solution was cooled from 313 to 296 K toward the solution critical point at ∼294 K for this CO_2 density ($\rho^* = \rho/\rho_C = 0.8$).

Neat CO_2 and CHF_3 fluids are electronically nonresonant (i.e., transparent) at the incident Ti:sapphire optical frequency (∼800 nm) both in a one- and in a two-photon absorption sense. However, this anomalous, autocorrelation-shaped signal was also observed for these samples in a dichroic pump−probe experimental configuration. Transparent materials (i.e., optically nonresonant samples) exhibit only an asymmetric response due to a so-called coherence coupling term, arising from the linear chirp of the incident pulses in such nondispersed pump−probe responses.[25−27] The anomalous autocorrelation-shaped signal contribution was clearly evident in solutions of SC CO_2 with 20−25 mol % H_2 (Figure 1), as well as in neat SC CO_2, and liquid and SC CHF_3 at state points in the region of the critical regime. When neat SC CO_2 was cooled to just below the critical point, the resulting vapor and liquid phases no longer exhibited this anomalous feature. Only the normal instantaneous nonresonant electronic and Raman active nuclear responses were observed in these OHD responses. The behavior in CHF_3 was somewhat different. This anomalous autocorrelation-shaped feature was strong in the SCF and, in contrast to CO_2, was also clearly evident in the liquid CHF_3 formed just below the critical point. We note that normal liquids (e.g., chloroform) in the identical femtosecond OHD−OKE experimental setup showed no evidence of this additional signal contribution. This novel nonresonant response can be understood in terms of the acoustic properties of these near critical fluids as discussed next.

Characterization of the Anomalous Signal. *OHD $P^{(3)}$ Signal.* The pump and probe pulse intensity dependence of the anomalous, autocorrelation-like feature is demonstrated in Figure 3. Log−log plots of the $t = 0$ signal intensity of liquid phase CHF_3 ($T = 294$ K and $\rho^* = 1.51$) in a two-beam pump−probe (dichroic) configuration as a function of the pump and pulse beam intensities are displayed in Figure 3. The resulting slopes of a linear best fitting procedure, 1.007 ± 0.012 and 1.038 ± 0.009 for the pump and probe dependent signals, respectively, establish that this nonlinear signal is linearly proportional to a third-order polarization ($P^{(3)}$) effect. In addition, this experimental configuration readily allows for the relative polarization dependence of the observed signal to be observed via $\lambda/2$ wave plate rotation. The observed in-phase response was largest for the parallel orientation of the pump and probe beam polarizations.

The optical heterodyne detected nature of these signals is demonstrated by the responses shown in Figure 4. The bire-

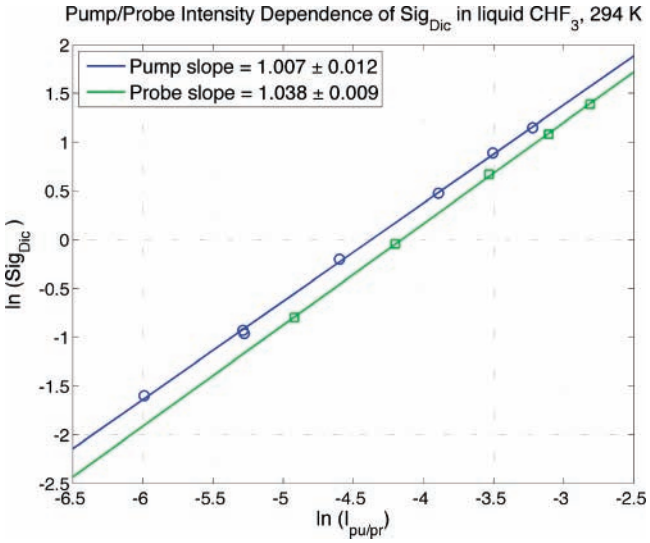

Figure 3. Log of the autocorrelation-like dichroic response of liquid phase CHF_3 (T = 294 K) as a function of the log of the pump and probe pulse intensity. Linear best fits to the observed intensity dependence are also shown in this figure and result in slopes of 1.007 ± 0.012 and 1.038 ± 0.0009 for the pump and probe intensity dependence, respectively.

fringent ($\phi_{LO} = \pi/2$) and dichroic ($\phi_{LO} = 0$) signals of SC CHF_3 (T = 305.5 K and ρ^* = 1.20) in the standard OHD−OKE configuration[11,12] are displayed in Figure 4b. As seen in this figure, the sign of both the birefringent and the dichroic CHF_3 signals flips as the local oscillator phase is shifted by π, keeping the LO field magnitude constant. The responses in the $t >$ 75 fs region in Figure 4b have been amplified by a factor of 50 (and the dichroic signals offset by −0.14 au) to more clearly show the relatively weak nuclear responses in these CHF_3 OHD birefringent signals and the absence of the nuclear responses in the corresponding OHD dichroic signal. Since no nuclear contributions are evident in the OHD dichroic response, the large autocorrelation-like feature at $t = 0$ cannot be attributed to leakage from the birefringent response. At this state point (T = 305.5 K and ρ^* = 1.20), the CHF_3 dichroic response is about one-third that of the birefringent response in this transparent sample. Furthermore, dichroic pump−probe responses due to linearly (odd order) chirped ultrafast pulses exhibit an asymmetric dispersive-like response centered at $t = 0$ in nonabsorbing materials.[26,28] The incident ~800 nm oscillator pulses used for these displayed measurements have a ~1.4 × transform limited pulse width (22 fs) and thus have sufficient phase modulation to result in such a dichroic feature in a pump−probe configuration that must be completely dwarfed by these large dichroic CHF_3 responses (Figure 4a,b). Thus, the intensity dependence and LO field phase dependence unequivocally establish that the large anomalous signals are optical heterodyned detected complex third-order polarization responses generated by these near critical fluids. This electronically nonresonant system generates real and imaginary $P^{(3)}$ amplitude components in these near critical point fluids. Finally, as noted previously, the anomalous $t = 0$ signal shown in Figure 4b is clearly π out-of-phase with the usual impulsively excited birefringent CHF_3 Raman nuclear and nonresonant instantaneous electronic responses that must arise from the inherent response functions for these processes given the phase matching constraints of the current two-beam experimental setup.

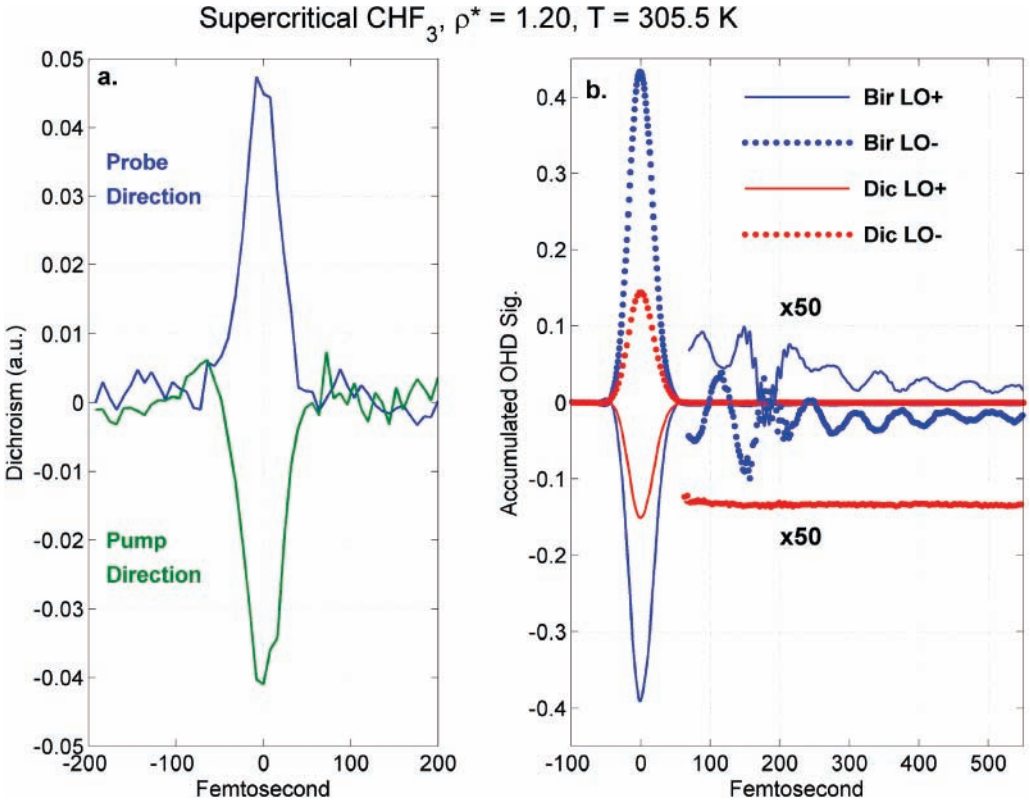

Figure 4. (a) Simultaneous dichroic signals of SC CHF_3 (ρ^* = 1.20, T = 305.5 K) in pump and probe directions. (b) Local oscillator (LO) dependence of the birefringent and dichroic responses of SC CHF_3. The nuclear response region after 75 fs has been amplified by 50× to demonstrate the magnitude of the accumulated OHD signal and to show that the dichroic response does not result from experimental leakage of the birefringent signal. The amplified (50×) $t >$ 75 fs dichroic has been displaced down 0.14 units for viewing purposes. The + (−) LO is indicated by solid (dashed) lines showing how the accumulated acoustic response is π out-of-phase with the CHF_3 birefringent Raman nuclear response.

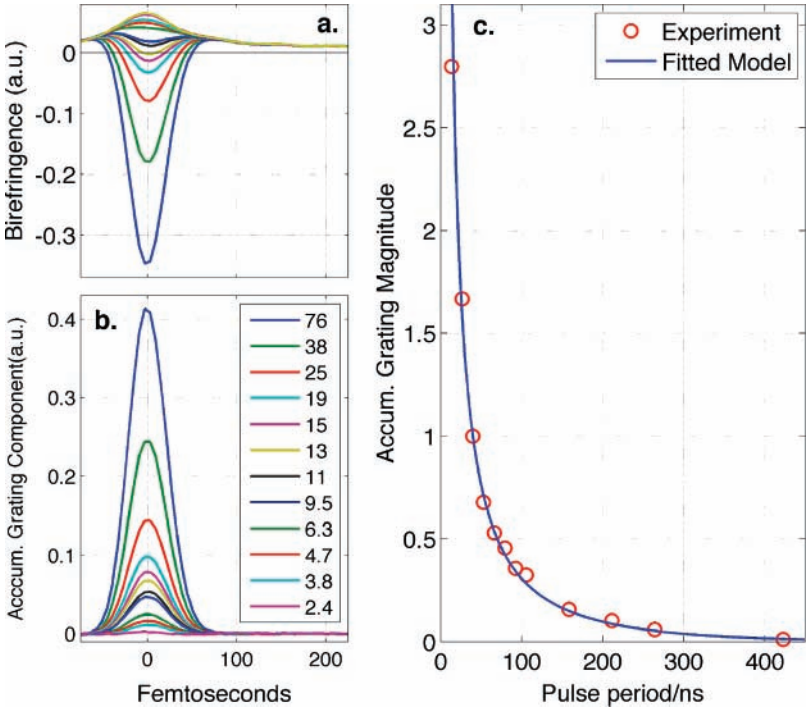

Figure 5. (a) Repetition rate dependence of the CHF_3 liquid ($\rho^* = 1.51$, $T = 294$ K) birefringent response normalized for incident number of pulses. (b) Repetition rate dependent part of the birefringent response shown in panel a. The laser pulse repetition rate in MHz is shown in the legend. (c) Experimental and fitted functional model form of the OHD accumulated signal intensity as a function of laser pulse period (inverse repetition rate). The one fitting parameter, apart from an overall scaling factor fixed by the 39.5 ns point, is the sound decay time (τ_a), determined by the best fit to be 127 ± 13 ns.

An additional characterization of the $t = 0$ dichroic signal is illustrated in Figure 4a. When the pump and probe beams are double chopped, lock-in detection at the sum frequency allows the energy changes in the transmitted pump and probe beams to be simultaneously measured. The pump and probe beams exhibit equal but opposite signed energy changes (bleach/absorption) in the dichroic responses of SC CHF_3 ($\rho^* = 1.20$ and $T = 305.5$ K) (Figure 4a). Such zero net energy gain is to be anticipated for a totally nonresonant (electronic and nuclear) response.

Pulse Repetition Rate Dependence. In one attempt to identify the nature of these OHD $P^{(3)}$ signals, we measured the OHD−OKE responses of near critical CO_2 and CHF_3 excited by laser pulses at ~800 or ~600 nm resulting from a regeneratively amplified laser system operating at 250 kHz. The OHD responses of near critical CO_2 and CHF_3 obtained with these excitation sources exhibited a normal type of birefringent (instantaneous nonresonant electronic and Raman nuclear) and dichroic (weak dispersive-shaped) responses in agreement with our previous OHD−OKE studies of near critical CO_2.[12] Comparison of signals obtained with these different laser sources established that this anomalous $t = 0$ feature was not due to beam characteristics such as excitation wavelength, pulse energy, pulse bandwidth, beam mode structure, or experimental artifacts (e.g., lenses, laser scatter, and sample cell). However, the pulse period was one remaining difference between these two excitation sources: 76 MHz (13.2 ns period) versus 250 kHz (4000 ns period).

The origin of this novel OHD $P^{(3)}$ effect in near SC fluids was unequivocally revealed when a pulse picker was used to systematically reduce the repetition rate of the incident pump and probe pulses from 76 MHz ($T = 13.2$ ns) to 2.4 MHz ($T = 421$ ns). The laser repetition rate dependence of the birefringent response of liquid fluoroform ($T = 294$ K and $\rho^* = 1.51$) is shown in Figure 5a. These signals have been normalized for average incident power effects due to the repetition rate reduction, and thus, the nuclear $t > 0$ Raman responses are all coincident as expected. In contrast, the magnitude of the $t = 0$ autocorrelation-like feature is strongly dependent on the laser repetition rate in this frequency range. This contribution to the OHD birefringent response dramatically decreases in magnitude as the period between pulses is varied from tens to hundreds of nanoseconds in this near critical CHF_3 sample. This repetition rate dependence in the 76 to 2.375 MHz range is more clearly evident in Figure 5b where the normal electronic and nuclear response has been removed from the average power corrected observed birefingent signals displayed in Figure 5a. As the interpulse delay (T) is increased from 13.2 to 421 ns, the signal monotonically but nonlinearly decreases with T and is virtually undetectable for delays on the order of 0.5 μs and longer at this state point in CHF_3. Thus, the observed OHD signal in these SC fluids is an accumulated signal whose observation is dependent on a relaxation phenomenon that must fall in the time scale of hundreds of nanoseconds and hence was not observed with 250 kHz laser pulses of the regenerative amplified system where $T = 4$ μs. As mentioned previously, heterodyne detected accumulated photon echo signals were readily observed when the excitation pulse cycle is short as compared to a bottleneck population decay time effectively amplifying the $P^{(3)}$ response at least for solid state materials.[21−23]

SCFs and OHD Accumulated Acoustic Gratings. *Phase Matching Considerations.* In most previous reports of optically generated longitudinal acoustic gratings,[2−7,29,30] the time dependence of the acoustic standing wave with wavevector $\mathbf{q}$ ($|\mathbf{q}| = |k_{pu1} - k_{pu2}|$) produced by the intensity interference pattern from two temporally and spatially co-incident pump pulses (k_{pu1} and k_{pu2}) is measured by the reflection efficiency of a probe laser incident in the sample overlap region (k_{pr}) scattered at some new angle as a function of delay time from the pair of pump pulses. The radiated response field or reflection satisfies the

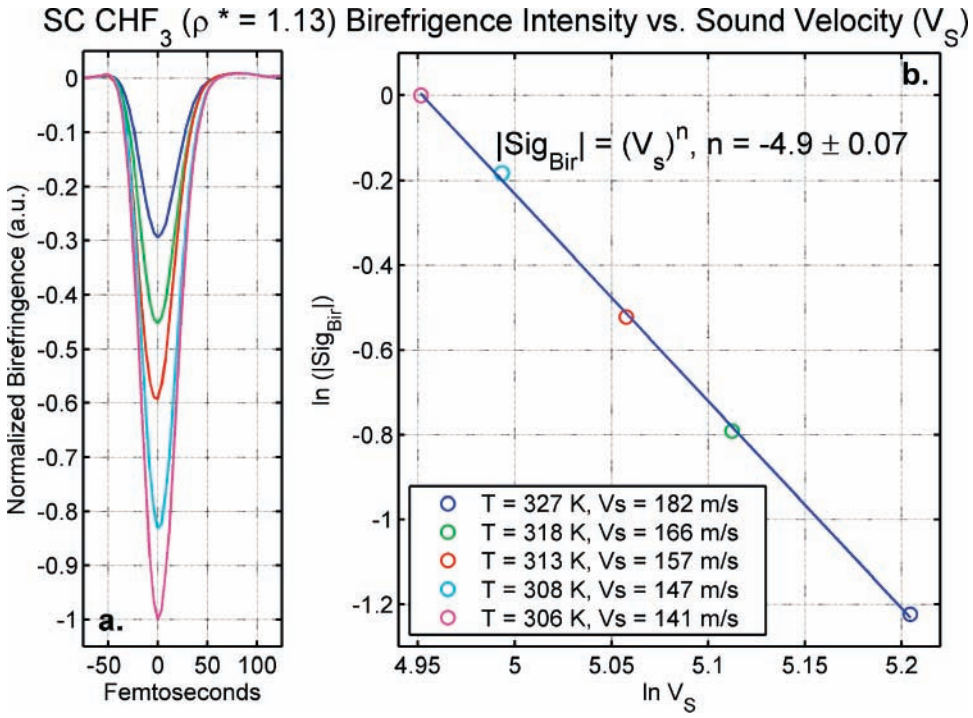

Figure 6. (a) Birefringent response of SC CHF_3 ($\rho^* = 1.13$) at isochoric conditions as a function of temperature over the range of 306 to 327 K. (b) Sound velocity for these temperatures is indicated in the legend box. A plot of the ln of the birefringent signal magnitude as a function of the ln of the sound velocity is best fit to a straight line with a slope of -4.9 ± 0.07.

Bragg condition in the previously dark $k_{pu1} - k_{pu2} - k_{pr}$ direction and is thus a homodyne ($|P^{(3)}|^2$) generated response.

In contrast, the acoustic grating resulting in the signal reported here can only be produced when the pump and probe pulses are temporally overlapped, resulting in the acoustic response with wavevector $|\mathbf{q}| = |k_{pu} - k_{pr}|$. Given the two-beam geometry of this experimental configuration, this is the only combination of incident fields that could result in an acoustic grating response. This two-beam origin for the acoustic grating is consistent with the observation that the acoustic grating based signal is largest for parallel orientations of the pump and probe electric vectors. Presumably, electrostriction is the dominant mechanism for coupling the optical fields to the acoustic response in these nonabsorbing fluids,[31] as discussed previously. Since the observed third-order signal polarization is heterodyning with the probe pulse when the signal is detected in the probe direction, the third interaction must be due to a pump field by phase matching constraints. Hence, the observed signal can only be generated during the time the pump and probe pulses are overlapped, and thus, the acoustic response has the temporal profile of the intensity autocorrelation function. A time-resolved acoustic response in this configuration would require two grating excitation field interactions separated by the relevant time scale to probe the acoustic response: here in the 10−100 ns regime. However, during data acquisition, the signal at each time step is averaged over a ~100 ms period typically, and thus, when the acoustic response relaxation time is of the order of the pulse period (T), there is a sufficient number of pulses to build up a steady state grating population and observe an accumulated acoustic response.

Sound Decay Rate Dependence. The integrated intensity of the accumulated acoustic OHD birefringent signals of CHF_3 shown in Figure 5a are plotted as a function of the interpulse spacing (pulse period, T) in Figure 5c. If the acoustic grating formed by the interference pattern of a pump and probe field decays exponentially with time constant, τ_a, due to sound absorption, then the amplitude of the accumulated OHD signal due to pulses spaced by period T and exponentially damped should build up according to

$$S(T, \tau_a) \propto \sum_{n=1}^{\infty} e^{-nT/\tau_a} = \frac{e^{-T/\tau_a}}{1 - e^{-T/\tau_a}} \quad (4)$$

When the functional form given by eq 4 is fit to these repetition rate dependent experimental intensities, an excellent, one parameter (aside from an overall scaling constant) fit is obtained for $\tau_a = 127 \pm 13$ ns as seen in Figure 5c. The decay rate due to sound absorption τ_a is given in terms of the sound absorption coefficient, α, and the speed of sound, V_S, by

$$\tau_a = \frac{1}{\alpha V_S} = \frac{\Lambda^2}{(\alpha \nu^{-2}) \upsilon_S^3} \quad (5)$$

The second equality follows from the sound propagation relation $\Lambda\nu = V_S$. As discussed previously, the quantity $\alpha\nu^{-2}$ is the constant noted for sound attenuation descriptions and has been found, for example, to be a constant for near critical CHF_3 in the high ($\omega > 150$ MHz) angular frequency regime.[5] If we use values for $\alpha\nu^{-2}$ (4×10^{-13} s^2 cm^{-1}) and υ_S (183 m/s) reported for fluoroform at similar densities and temperatures,[5] then eq 5 yields a value of $\tau_a = 117 \pm 20$ ns for the experimental conditions of this measurement ($\lambda = 792$ nm, $\theta = 8.3°$, and $\Lambda = 5.16$ μm). This sound decay time is in excellent agreement with that determined by the fit to the pulse period dependence of the OHD accumulated acoustic response (Figure 5c), 127 ± 13 ns. Furthermore, this acoustic relaxation time scale is nearly an order of magnitude longer than the interpulse period of the Ti:sapphire oscillator (13.2 ns) and is thus consistent with the observation of an accumulated acoustic response in this SCF.

Sound Velocity Dependence. The very sensitive dependence of the strength of this OHD accumulated acoustic signal on sound velocity is illustrated in Figure 6. The birefringent response of SC CHF_3 ($\rho^* = 1.13$) as a function of temperature

in the range of 306−327 K in shown in Figure 6a. Over this modest 6% temperature range, the observed birefringent acoustic signal intensity changes by more than a factor of 3. A log−log plot of the CHF_3 accumulated OHD birefringent peak signal intensity as a function of the sound velocity at each corresponding temperature[14] is given in Figure 6b. As seen in Figure 6b, an excellent best-fit linear dependence is found in this log−log plot, yielding a slope of -4.9 ± 0.07. Thus, empirically, we find that this accumulated OHD birefringent ($\phi_{LO} = \pi/2$) acoustic signal is inversely proportional to the speed of sound to the fifth power (V_S^{-5}).

The V_S^{-5} power dependence for these accumulated signals can be rationalized in terms of the overall efficiency of the electrostriction process and the sound velocity dependence of the sound decay time. Following Boyd,[31] the efficiency of grating production owing to the change in density, $\Delta\rho$, created by electrostrictive forces due to optical frequency fields E, is given by

$$\Delta\rho = \rho C_S \gamma_e \frac{\langle EE \rangle}{8\pi} \tag{6}$$

where $C_S = (\partial\rho/\partial\rho)/\rho$ is the compressibility evaluated at constant entropy and $\gamma_e = \rho(\partial\epsilon/\partial\rho)$ is the electrostriction constant. The resulting nonlinear polarization is proportional to this change in density.[2,6] The constant entropy compressibility can be defined in terms of the density and speed of sound: $C_S = 1/(\rho v_S^2)$.[2,31] Thus, as the sound velocity decreases, the efficiency of electrostriction driven acoustic grating generation increases quadratically. The nonlinear index of refraction due to a time averaged electric field resulting from the fringes of an interference pattern produced by the superposition of coherent radiation fields has also been shown to vary inversely proportionally to the square of the sound velocity.[32]

Furthermore, for the accumulated OKE signals, the expected amplification due to the pulse train period (T) being shorter than the sound decay time (τ_a) is described by eq 4. When the exponentials in this expression are expanded and evaluated for $\tau_a > T$, the following relationship is obtained when τ_a is given in terms of V_S (eq 5):

$$S(T, \tau_a) \propto \frac{e^{-T/\tau_a}}{1 - \epsilon^{-T/\tau_a}} \approx \frac{\tau_a}{T} = \frac{\Lambda^2}{T(\alpha\nu^{-2})v_S{}^3} \tag{7}$$

When this sound velocity dependence is combined with the v_S^{-2} value due to compressibility scaling the electrostrictive opto-acoustic coupling contribution (eq 6), a $1/V_S^5$ dependence is obtained. For the data shown in Figure 6, $\tau_a = 120$ ns for CHF_3 at $\rho^* = 1.13$, which is about an order of magnitude longer than the pulse period for 76 MHz pulses ($T = 13.2$ ns), and thus, expanding the exponentials (eq 7) is a reasonable approximation (5% error).

Complex $P^{(3)}$ Response. As discussed previously (see Figure 4b), both in-phase (dichroic) and $\pi/2$ out-of-phase (birefringent) OHD accumulated acoustic grating signals are observed in the OKE configuration for these nominally transparent SCFs. The birefringent signal is found to be larger than the corresponding dichroic signal for the same LO oscillator strength at the state points studied. However, the ratio of these OHD detected real and imaginary $P^{(3)}$ based components exhibits a systematic trend with temperature. The ratios (by area) of the observed dichroic to birefringent signals (S_{dic}/S_{bir}) of SC CHF_3 ($\rho^* = 1.2$) are plotted as a function of temperature and sound velocity in Figure 7. As seen in Figure 7, the magnitude of the accumulated dichroic signal in SC CHF_3 decreases relative to the corresponding birefringent signal as the temperature is reduced in the SC region toward the CHF_3 critical temperature ($T_C = 299.3$ K). The sound velocity for this SC fluid is nearly linearly dependent on temperature in this SC region and decreases by ~25% as the temperature is reduced from 318 to 305 K.[14] Within this albeit relatively limited temperature range and the precision of these measurements, the relative magnitudes of dichroic and birefringent intensities, S_{dic}/S_{bir}, exhibit a linear dependence on the sound velocity.

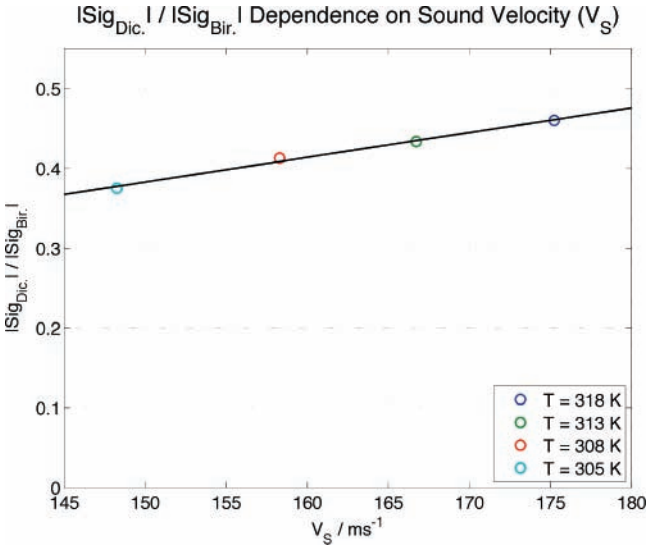

Figure 7. Relative magnitude of the dichroic to birefringent response of liquid CHF_3 ($\rho^* = 1.2$) as a function of the speed of sound (V_S).

Only a weak antisymmetrically shaped response, arising from the phase modulation of the pulse envelope, would be anticipated for these electronically nonresonant OHD dichroic responses around the pulse overlap region.[26−28] However, for these accumulated OHD grating responses, we attribute the complex character of the third-order polarization amplitude to the motion of the acoustic standing wave on the time scale of the grating population buildup. In the previous study of an accumulated thermal grating response generated in an absorbing dye solution,[25] the rapid flow of the solution caused the pure phase gratings to acquire a complex character when the thermal diffusion grating relaxation time was of the order of the time interval between pulses. Hence, for a rapidly flowing solution, the signal field acquired a time dependent phase factor given by $\exp(i\mathbf{q}v\ \sin(\theta)(t - t'))$, where $v\ \sin(\theta)$ is the velocity component perpendicular to the grating direction and $(t - t')$ is the time interval between successive pulse train interactions.[25] This is just the usual spatial phase factor that results when two idealized plane waves interact with a medium. For pump−probe studies at short times, the translational (diffusive) motion of such a flowing sample is generally too slow to affect the observed nonaccumulated responses.

The standing sound wave produced in the interference region of the pump−probe laser beams decays into two moving sound waves traveling apart from each other at a rate that is proportional to the sound velocity.[1] Thus, in analogy to the flowing thermal generated gratings stated previously, this spatially dependent phase factor can be described by $\exp(i\phi)$, where $\phi \propto \mathbf{q}V_S(t - t')$. The exact magnitude of this phase factor is dependent on finite beam size effects.[30,33] However, a consequence of this sound velocity dependent phase is that the ratio of the dichroic (in-phase) to birefringent ($\pi/2$ out-of-phase) signal magnitudes (S_{dic}/S_{bir}) is predicted to be proportional to $\tan\phi$, and for relatively small angles, $\tan\phi \approx \phi$. For the SC

CHF_3 data shown in Figure 7, $S_{dic}/S_{bir} = \sim 0.4$; thus, ϕ is ~ 0.38 rad following the previous discussion, and $\tan \phi \approx \phi$ is a good approximation. The observed S_{dic}/S_{bir} linear dependence on the sound velocity in this regime exhibited in Figure 7 is consistent with such a ϕ value. Thus, in contrast to the demonstrated (Figure 6b) V_S^{-5} dependence of the OHD accumulated birefringent responses of the near critical fluid, the corresponding observed dichroic response is inversely proportional to the fourth power of the sound velocity.

Conclusion

A new near critical point optical effect, most directly due to the enhanced compressibility of fluids in this thermodynamic region, is reported here. Large, accumulated, electrostrictively coupled acoustic responses are readily observed in the OHD−OKE two-beam configuration employing a high repetition rate (76 MHz) laser in near critical CO_2 and CHF_3. By phase matching constraints, this accumulated $P^{(3)}$ response is only observed when the pump and probe pulses are temporally overlapped and hence has the appearance of a greatly enhanced nonresonant electronic response at the incident colors used here. This feature is π out-of-phase with respect to the normal nuclear and nonresonant electronic responses of transparent liquids and appears in both the dichroic and the birefringent OHD responses. This complex character is proportional to the sound velocity. Experimental evidence is presented, which establishes the accumulated, optical heterodyne $P^{(3)}$ nature of these signals.

The large magnitude of this accumulated response is probably most fundamentally attributable to the singularity in the compressibility of a fluid at the critical point, which results in a minimum for the sound velocity (eq 2) and the relatively long acoustic relaxation time ($\sim 10^2$ to 10^3 ns) as compared to the pulse period time scale (13.2 ns). Remarkably, the observed accumulated acoustic birefringent signal in SC CHF_3 is found to be inversely dependent on the sound velocity to the fifth power and must significantly account for the apparent absence of this signal in normal liquids. Despite the difference in sound attenuation, α/ν^2 (see Table 1), the estimated (eqs 6 and 7) relative accumulated acoustic response of SC fluoroform ($\rho^* = 1.2$, $T = 307$ K, and $V_S = 146$ m/s) is more than 300 times larger than that of liquid chloroform near room temperature ($\rho^* = 2.99$, $T = 295$ K, and $V_S = 995$ m/s), for example, arising from the V_S^{-5} dependence. Hence, to the extent that these acoustic parameters are typical of most normal liquids, this accumulated signal probably does not contribute to the OKE measurements of normal (non-critical) liquids reported in the past 10−20 years obtained with typical Ti:sapphire oscillator only systems. Furthermore, although this accumulated signal is readily observed in SC and liquid CHF_3, and SC CO_2, as discussed previously, the corresponding accumulated signal was not evident in near critical liquid CO_2. We attribute the apparent absence of this signal in liquid CO_2 to the high-order dependence on the sound velocity. The fifth power of the relative sound velocities of liquid CO_2 ($\rho^* = 1.7$, $T = 293$ K, and $V_S = 350$ m/s) and SC CO_2 ($\rho^* = 0.8$, $T = 308$ K, and $V_S = 185$ m/s) alone accounts for a factor of 25 difference in relative signal strength detected in the OHD birefringent configuration. Assuming that the sound attenuation does not vary significantly in this near critical region (except within ~ 1 K of the critical point),[18] such a reduced accumulated response would not be evident as compared to the normal electronic and nuclear birefringent response of liquid CO_2. No evidence of these anomalously strong autocorrelation-like features were reported in a previous study of fluoroform OKE responses excited by ultrafast, high repetition rate 25 fs Ti:sapphire oscillator pulses.[34] However, in contrast to the detection employed here, a shaker was used to rapidly acquire the entire response, and then multiple traces were averaged, thus avoiding the population accumulation and subsequent pulse readout.

While the data shown here serve to characterize the more salient features of this novel optically generated acoustic response, subsequent observations are planned to help develop a more rigorous theoretical description of this phenomenon and explore potential applications for this large system response. The magnitude of these signals in near critical fluids suggests that by taking advantage of their large compressibilities, these materials may be used as highly efficient light modulators or deflectors. Furthermore, given the relative ease of the required experimental configuration (i.e., two-beam as compared to three-beam transient grating configuration), and the observed fifth power sound velocity dependence, quantitative analysis of this optical phenomenon has the potential for being an additional sensitive measure of acoustic properties and thermodynamic state points of SCFs and near critical mixtures. Future studies will contrast the more standard three beam homodyne transient grating response in these SC fluids with the observed accumulated OHD responses, determine measures of the grating efficiency, explore this phenomenon for other SCFs, and make measurements of both dichroic and birefringent accumulated OHD responses over a larger range of state points, including closer to the critical point where the sound attenuation constant (α/ν^2) dramatically increases.[16,18] Such observations will allow a more quantitative treatment of this accumulated acoustic nonlinear optical effect and a useful test of equation of states particularly for less well-characterized SC fluid mixtures.

Acknowledgment. The support of the National Science Foundation (Grant CHE-0310497) and the Boston University Photonics Center is gratefully acknowledged.

References and Notes

(1) Eichler, H. J.; Gunter, P.; Pohl, D. W. *Laser-Induced Dynamic Gratings*; Springer-Verlag: Berlin, 1986.

(2) Nelson, K. A.; Lutz, D. R.; Fayer, M. D. Laser induced phonon spectroscopy. Optical generation of ultrasonic waves and investigation of electronic excited-state interactions in solids. *Phys. Rev. B: Condens. Matter Mater. Phys.* **1981**, *24*, 3261−75.

(3) Nelson, K. A.; Miller, R. J. D.; Lutz, D. R.; Fayer, M. D. Optical generation of tunable ultrasonic waves. *J. Appl. Phys.* **1982**, *53*, 1144−49.

(4) Miller, R. J. D.; Casalegno, R.; Nelson, K. A.; Fayer, M. D. Laser-induced ultrasonics: A dynamic holographic approach to the measurement of weak absorptions, optoelastic constants, and acoustic attenuation. *Chem. Phys.* **1982**, *72*, 371−79.

(5) Kimura, Y.; Kanda, D.; Terazima, M.; Hirota, N. Application of the transient grating method to the measurement of transport properties for high pressure fluids. *Ber. Bunsen-Ges. Phys. Chem.* **1995**, *99*, 196−203.

(6) Hubschmid, W.; Hemmerling, B.; Stampanoni-Parariello, A. Rayleigh and Brillouin modes in electrostrictive gratings. *J. Opt. Soc. Am. B* **1995**, *12*, 1850−54.

(7) Govoni, D. E.; Booze, A.; Sinha, A.; Crim, F. F. The non-resonant signal in laser induced grating spectroscopy. *Chem. Phys. Lett.* **1993**, *216*, 525−29.

(8) Crimmins, T. F.; Stoyanov, N. S.; Nelson, K. A. Heterodyned impulsive stimulated Raman scattering of phonon-polaritons in $LiTaO_3$ and $LiNbO_3$. *J. Chem. Phys.* **2002**, *117*, 2882−96.

(9) Thomsen, C.; Grahn, H. T.; Maris, H. J.; Tauc, J. Picosecond interferometric technique for study of phonons in the brillouin range. *Opt. Commun.* **1986**, *60*, 55−58.

(10) Peng, J.; Castonguay, T.; Coker, D. C.; Ziegler, L. D. The rotational Raman responses of H_2 in supercritical CO_2. *J. Chem. Phys.*, submitted.

(11) Lotshaw, W. T.; McMorrow, D.; Thantu, N.; Melinger, J. S.; Kitchenham, R. Intermolecular vibrational coherence in molecular liquids. *J. Raman Spectrosc.* **1995**, *26*, 571−83.

(12) Zhou, Y.; Constantine, S.; Harrel, S.; Gardecki, J. A.; Ziegler, L. D. The femtosecond birefringence of CO_2: From the high pressure gas to the liquid phase. *J. Raman Spectrosc.* **2000**, *31*, 85−94.

(13) Hirchfelder, J. O.; Curtiss, C. F.; Bird, R. B. *Molecular Theory of Gases and Liquids*; John Wiley and Sons, Inc.: New York, 1954.

(14) *NIST Chemistry WebBook, NIST Standard Reference Database No. 69*, June 2005 release; NIST: Washington, DC, 2005; http://webbook.nist.gov/chemistry/.

(15) National Physical Laboratory. *Kaye and Laby Tables of Physical and Chemical Constants*; National Physical Laboratory: Middlesex, U.K.; http://www.kayelaby.npl.co.uk/general_physics/2_4/2_4_1.html.

(16) Schneider, W. G. Ultrasonic absorption in the critical temperature region. *J. Chem. Phys.* **1950**, *18*, 1300.

(17) Herget, C. M. Ultrasonic velocity in carbon dioxide and ethylene in the critical region. *J. Chem. Phys.* **1940**, *8*, 537−42.

(18) Zevnik, L.; Babic, M.; Levec, L. Ultrasound speed and absorption study in near-critical CO_2: A sensor for high-pressure application. *J. Supercrit. Fluids* **2006**, *36*, 245−53.

(19) Bhatia, A. B. *Ultrasonic Absorption*; Clarendon Press: Oxford, 1967.

(20) Quinn, J. The absorption of ultrasonic waves in benzene. *J. Acoust. Soc. Am.* **1946**, *18*, 185−89.

(21) Hesselink, W. H.; Wiersma, D. A. Picosecond photon echoes stimulated from an accumulated grating. *Phys. Rev. Lett.* **1979**, *43*, 1991−94.

(22) Hesselink, W. H.; Wiersma, D. A. Optical dephasing and vibronic relaxation in molecular mixed crystals: A picoseond photon echo and optical study of pentacene in naphthalene and *p*-terphenyl. *J. Chem. Phys.* **1980**, *73*, 648−63.

(23) Fuji, T.; Fukuda, H.; Hattori, T.; Nakatsuka, H. Femtosecond accumulated photon echoes excited by an incandescent lamp. *Opt. Commun.* **1996**, 104−08.

(24) Kuroda, T.; Minami, F.; Inoue, K.; Baranov, A. V. Accumulated photon echo in semiconductor microcrystalline quantum dots. *Phys. Rev. B: Condens. Matter Mater. Phys.* **1998**, *57*, 2077−80.

(25) Hayden, C. C.; Trebino, R. Coherent interactions in two-beam excited-probe absorption measurements. *Appl. Phys. B: Lasers Opt.* **1990**, *51*, 350−57.

(26) Ziegler, L. D.; Jordanides, X. J. Two-photon absorption resonance effects in the third-order response of transparent liquids. *Chem. Phys. Lett.* **2002**, *352*, 270−80.

(27) Palfrey, S. L.; Heinz, T. F. Coherent interactions in pump−probe absorption measurements: The effect of phase gratings. *J. Opt. Soc. Am. B* **1985**, *2*, 674−79.

(28) Ziegler, L. D.; Peng, J.; Constantine, S. Polarization specific ultrafast nuclear dichroic response: Raman spectral density recovery and coherent coupling effects. *Bull. Chem. Soc. Jpn.* **2002**, *75*, 1111−18.

(29) Stampanoni-Parariello, A.; Hemmerling, B.; Hubschmid, W. Electrostrictive generation of nonresonant gratings in the gas phase by multimode lasers. *Phys. Rev. A: At., Mol., Opt. Phys.* **1995**, *655*, 655−62.

(30) Yan, Y.-X.; Nelson, K. A. Impulsive stimulated light scattering. I. General theory. *J. Chem. Phys.* **1987**, *87*, 6240−56.

(31) Boyd, W. *Nonlinear Optics*; Academic Press: San Diego, 2003.

(32) Sutherland, R. L. *Handbook of Nonlinear Optics*; Marcel Dekker, Inc.: New York, 1996.

(33) Cummings, E. B.; Leyva, I. A.; Hornung, H. G. Laser-induced thermal acoustic (LITA) signals from finite beams. *Appl. Opt.* **1995**, *34*, 3290−302.

(34) Laurent, T. F.; Hennig, H.; Ernsting, N. P.; Kovalenko, S. A. The ultrafast optical Kerr effect in liquid fluoroform: An estimate of the collision-induced contribution. *Phys. Chem. Chem. Phys.* **2000**, *2*, 2691−97.